Available online at www.sciencedirect.com
ScienceDirect
Journal of the European Ceramic Society 31 (2011) 847–854
www.elsevier.com/locate/jeurceramsoc

Fabrication of wood-like porous silicon carbide ceramics without templates

Guangliang Liu [a,*], Peiyun Dai [a], Yanzhong Wang [b], Jianfeng Yang [a], Yabin Zhang [c]

[a] State Key Laboratory for Mechanical Behavior of Materials, Xi'an Jiaotong University, Xi'an 710049, PR China
[b] School of Materials Science and Chemical Engineering, Xi'an Technological University, Xi'an 710032, PR China
[c] Key Laboratory of Hollow Fiber Membrane Material and Membrane Process of Ministry of Education, Tianjin Polytechnic University, Tianjin 300160, PR China

Received 17 September 2010; received in revised form 15 November 2010; accepted 28 November 2010

Abstract

The porous silicon carbide ceramics with wood-like structure have been fabricated via high temperature recrystallization process by mimicking the formation mechanism of the cellular structure of woods. Silicon carbide decomposes to produce the gas mixture of Si, Si_2C and SiC_2 at high temperature, and silicon gas plays a role of a transport medium for carbon and silicon carbide. The directional flow of gas mixture in the porous green body induces the surface ablation, rearrangement and recrystallization of silicon carbide grains, which leads to the formation of the aligned columnar fibrous silicon carbide crystals and tubular pores in the axial direction. The orientation degree of silicon carbide crystals and pores in the axial direction strongly depends on the temperature and furnace pressure such as it increases with increasing temperature while it decreases with increasing furnace pressure.

Keywords: SiC; Porous ceramics; Microstructure; Processing

1. Introduction

In recent years, porous silicon carbide ceramics have attracted particular interest due to their unique properties such as low density, good thermal shock resistance, high mechanical properties and excellent chemical stability at elevated temperature, which make them suitable for a wide range of applications such as catalyst supports, filters for hot gas or molten metal, and high efficiency combustion burners.[1–3] The performances of porous silicon carbide, especially the mechanical properties are strongly dependent on their pore structures such as their pore size, distribution, interconnection between pores, and pore orientation. Thus, the preferred fabrication method should be able to allow the pore structure of ceramics controlled easily in order to optimize their properties.

Nowadays, many methods for the fabrication of the porous silicon carbide have been developed, such as polymer replication method,[4] processes based on the pore forming agents,[5,6] and biomorphic porous ceramics produced using natural plant as sacrificial templates.[7,8] Among these methods, the biomimicking method has recently received intensive attention since the biological structures usually exhibit some unique features of complex hierarchical cellular structures and open porous system.[9] Up to now, a number of natural plants are used as carbon source such as cellulose fibers (cellulose fiber felts, paper), wood, bamboo, and fruit residues.[10–14] Among these natural plants templates, wood are widely investigated because the wood-based SiC can retain the anisotropic, hierarchical and elongated tubular structure of wood that has optical properties from the viewpoint of the mechanical properties/density relationship and fluid transport.[15–19] The special structure and properties of wood are derived from the mechanism of wood formation[20–24]: water is a transport medium for minerals, gas, sugars, etc. by the short-range diffusion and long distance directional transport due to the gradient of the pressure and concentration formed by transpiration. The temperature affects the change of pressure (transpiration activity); further affect the availability and transport of materials, and the growth of wood. The preferred orientation growth of the anisotropic particles (ray and fusiform initial cells) in a porous (cellular) organization leads to the formation of wood structure. The familiar patterns of woods are known as the annual growth rings and fiber structure.

The wood-like SiC should be an ideal candidate for high-temperature exhaust filters, composites, corrosion-resistant

* Corresponding author. Tel.: +86 29 82663453; fax: +86 29 82667942.
E-mail address: liuguangliang555@126.com (G. Liu).

0955-2219/$ – see front matter © 2010 Elsevier Ltd. All rights reserved.
doi:10.1016/j.jeurceramsoc.2010.11.036

immobilization supports for bioactive substances.[25–27] However, the fabrication of wood-like silicon carbide is very complex and suffers from the problems of the limited selection of available natural templates, and silicon carbide ceramics produced inevitably contain some degree of silicon and residual carbon which induces the degradation of mechanical properties, and decreases the thermal and chemical stability at elevated temperature.[28,29]

In this study, we demonstrate a simple, innovative method for fabricating wood-like porous silicon carbide ceramics by high temperature recrystallization process. This method mimics the formation mechanism of the cellular structure of woods by controlling the experimental conditions. During high temperature sintering, the gradients of temperature, pressure and concentration in the graphite sagger result in the different rate of the decomposition, recrystallization and crystal growth of silicon carbide, such as the different pressure and concentration of gases in the axial direction are higher than that in the radial direction, which would allow the formation of aligned pores and silicon carbide crystals in the axial direction. The temperature gradient in the radial direction leads to the formation of ceramics lamellas that are similar to the wood-like rings. The formation mechanism and control of pore structure have been discussed.

2. Experiment

Starting materials used in our experiments were commercial grade silicon carbide powders (F180, Zaozhuang Liyuan Silicon Carbide Co., Ltd, Zaozhuang, China) with grain size (d_{50}) is 113.4 μm, specific surface area is 0.018 m^2/g and purity is 99.9%. Silicon carbide powders were added into the graphite saggers (inside diameter: 48 mm, depth: 100 mm, wall thickness: 3 mm). The height of silicon carbide powders in the graphite sagger was 70 mm and they were completely loose or vibrated to compact. Then the graphite sagger is covered by the graphite crucible (inside diameter: 100 mm, depth: 120 mm, wall thickness: 8 mm). The samples were sintered in medium frequency vacuum induction furnace (3.5 kHZ, Model ZGRS-160/2.55 Jinzhou Electric Furnace Co., Ltd., Jinzhou, China). The specimens were sintered in argon atmosphere with a heating and cooling rate of 50 °C/min. The maximum temperature difference in the axial direction of the graphite crucible is less than 3 °C. The specimens were sintered under different conditions, including: at different temperatures (1950 °C, 2050 °C, 2150 °C, 2250 °C and 2300 °C) for 2 h under the same furnace pressure 0.5×10^5 Pa; and at the same temperature 2250 °C under different furnace pressure (0.3×10^5 Pa, 0.4×10^5 Pa, 0.5×10^5 Pa, 0.6×10^5 Pa) for 2 h, respectively. The processing steps are schematically shown in Fig. 1.

The open porosity was determined by the Archimedes method, and kerosene was used as the liquid medium. The distribution of particle size was characterized by laser particle size analyzer (Model Rise-2008, Jinan Rise Science & Technology Co., Ltd., Jinan, China). The phase formation of specimens was analyzed by X-ray diffractometry (XRD, X'Pert PRO, PANalytical, Netherlands) using Cu Kα radiation. XRD patterns of

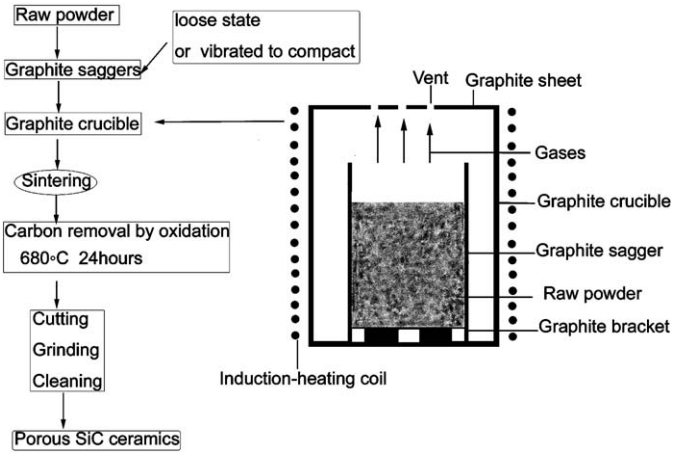

Fig. 1. The flow-chart of sample preparation.

samples were obtained in the 2θ range between 10° and 85° with a step of 0.01° and a scan speed of 10°/min. The microstructure of porous SiC ceramics such as the crystal morphologies, pore shapes were observed by scanning electron microscopy (SEM, Model JSM-6460, JEOL, Japan). Specimens were cut into the dimension of 5.0 mm × 5.0 mm × 30.0 mm to test the flexural strength via three-point bending test (Model WDT-10, Tianshui Hongshan Test Machine Accessories Factory, Tianshui, China) with a support distance of 25.0 mm and a cross-head speed of 0.5 mm/min.

3. Results and discussion

3.1. Macrostructure and microstructure

Fig. 2 shows the macro-appearance of samples sintered at 2300 °C for 2 h under the furnace pressure of 0.5×10^5 Pa in argon atmosphere. As can be seen, the rough surface in the radial

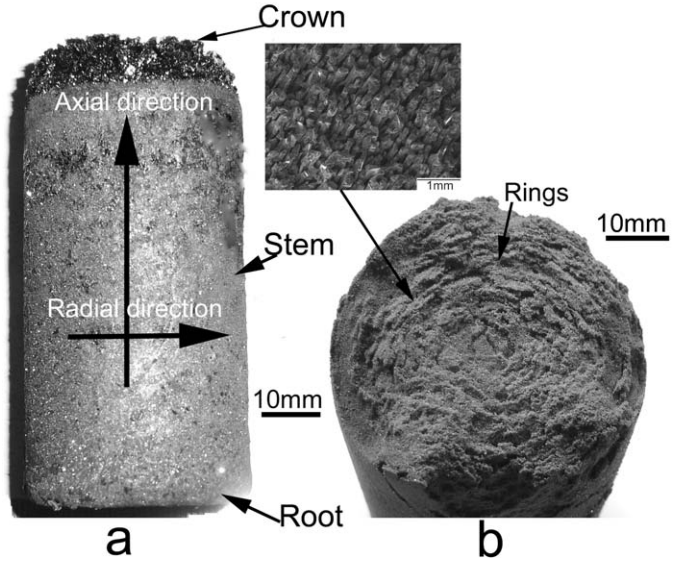

Fig. 2. The macro-appearance of samples sintered at 2300 °C for 2 h under 0.5×10^5 Pa: (a) the sintered samples and (b) the radial fracture surface.

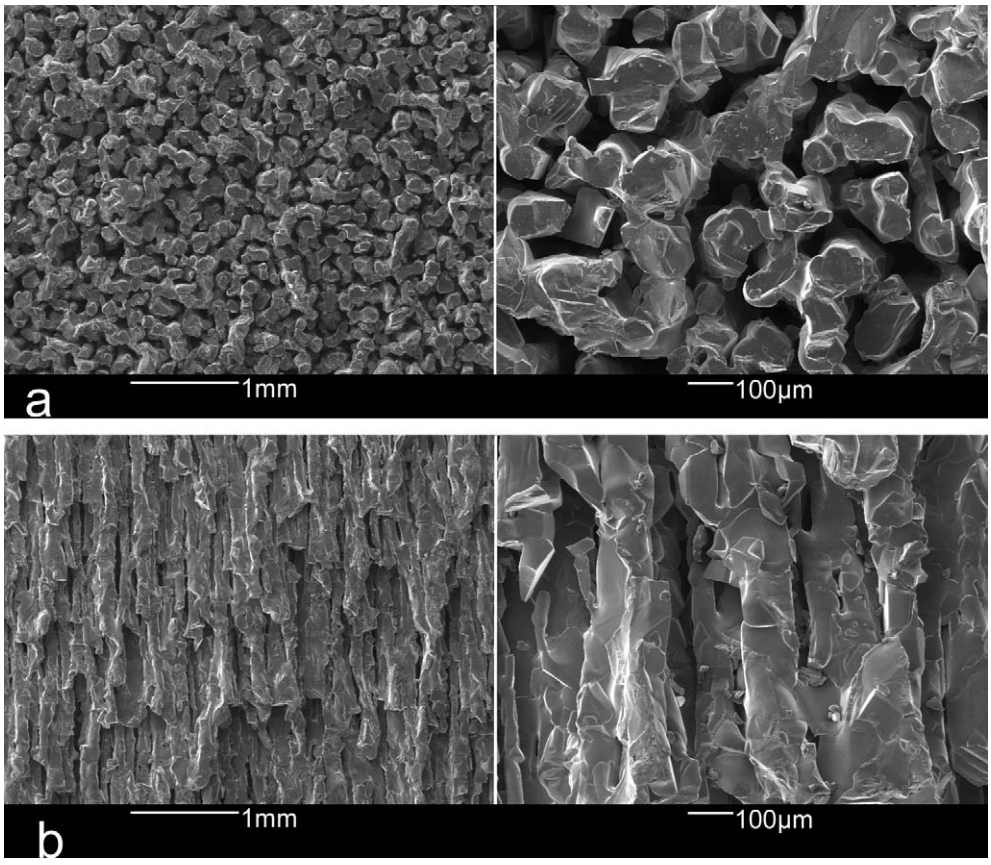

Fig. 3. The morphologies of sample (2300 °C for 2 h, 0.5 × 10^5 Pa): (a) the radial section surface and (b) the axial section surface.

fracture section displays wood-like rings, and there are a lot of flaky silicon carbide crystals in the crown. The microstructure of this sample was shown in Fig. 3. It shows that the porous silicon carbide consists of the highly aligned silicon carbide crystals and tubular pores that are located between them. The columnar silicon carbide crystals exhibit a fibrous structure which was parallel to the axial direction. The directional and tubular pores that are intercommunicating result in the formation of the long conducting channels, which was similar to the cellular structure of woods.

Fig. 4 shows the X-ray diffraction patterns in the axial and radial directions of samples. The phase can be identified as the pure alpha-SiC (6H). Comparing the intensities of the (0 0 0 1) peak for the axial and radial directions of samples and raw powder, the preferential orientation in (0 0 0 1) direction was exhibited, forming c-axis oriented grains. It suggests that the oriented growth of SiC crystals were in the axial direction during sintering, which was confirmed by the SEM images (Fig. 3).

3.2. The mechanism of reaction and structure formation

In this study, samples were heated by electromagnetic induction heating. The induction heating is comprised of three basic factors: electromagnetic induction, the skin effect, and heat transfer.[30,31] In order to obtain the uniform microstructure of samples in the axial direction, the electromagnetic field was controlled to be distributed in the graphite sagger to minimize the temperature gradient in the axial direction. The large temperature gradient in the radial of graphite sagger was formed due to the skin effect and heat transfer in loose porous samples.[31] The shape of graphite crucible used is columnar and similar to the wood stem. The radial temperature gradient leads to the formation the wood-like rings in Fig. 2.

According to references,[32,33] the decomposition of silicon carbide produces the gas mixture of Si, Si_2C and SiC_2 above

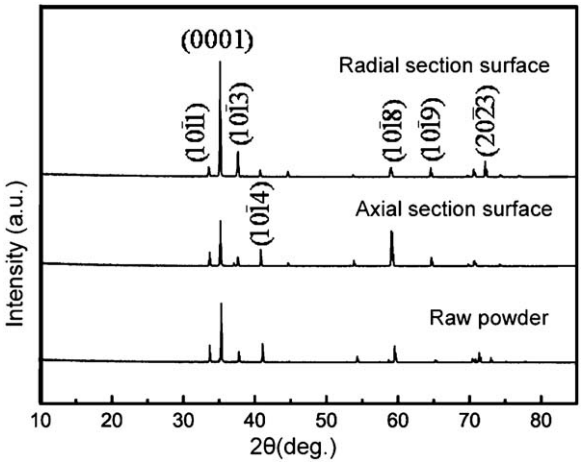

Fig. 4. XRD of sample (2300 °C, 0.5 × 10^5 Pa, 2 h) and raw powder.

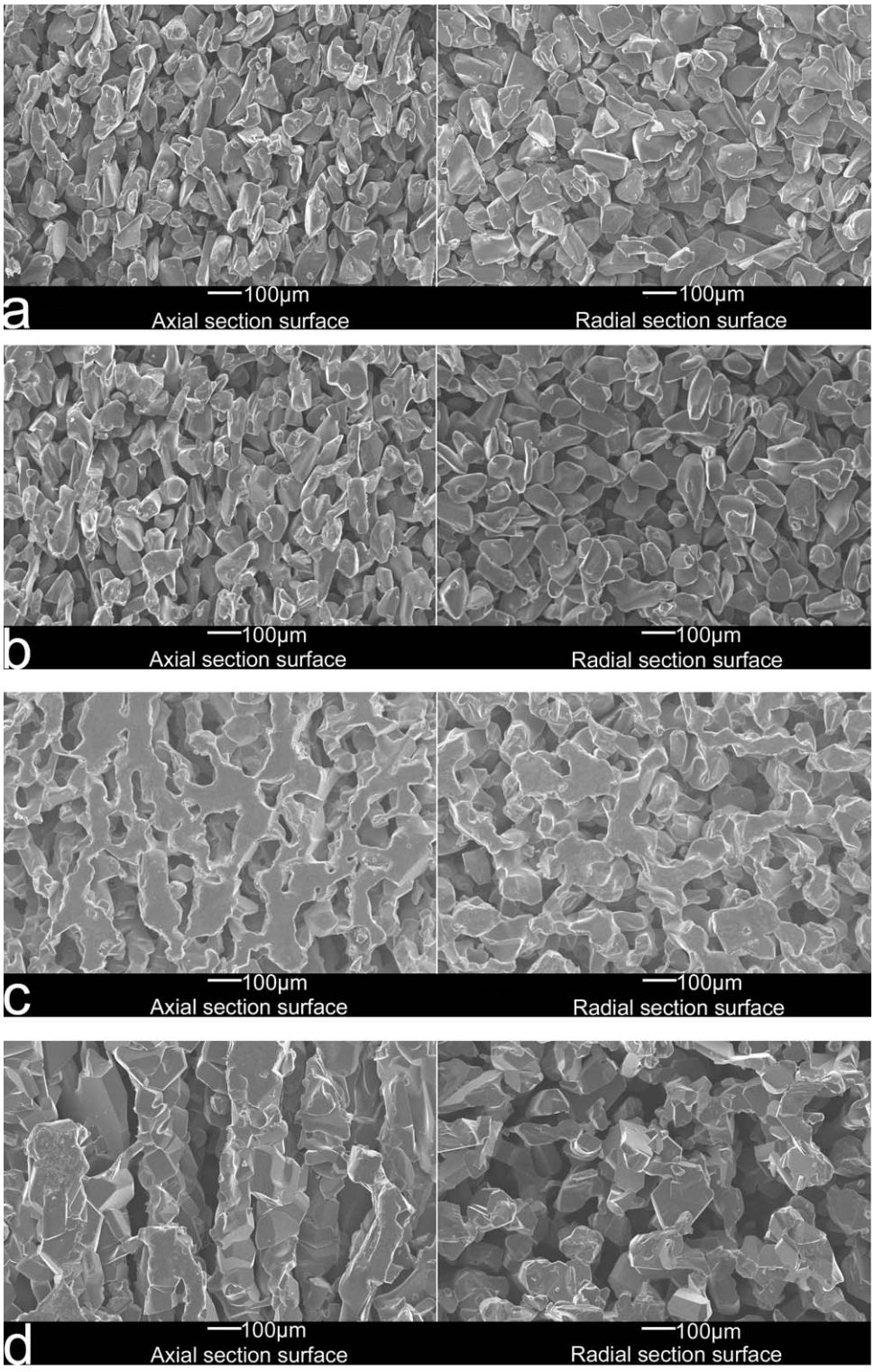

Fig. 5. The influence of temperature variation on the microstructure of samples (0.5×10^5 Pa, 2 h): (a) 1950 °C, (b) 2050 °C, (c) 2150 °C, and (d) 2250 °C.

1800 °C. The reactions are given as follows:

$$SiC\,(solid) \Leftrightarrow Si\,(gas) \uparrow + C\,(solid)) \quad (1)$$

$$2SiC\,(solid) \Leftrightarrow Si\,(gas) \uparrow + SiC_2\,(gas) \uparrow \quad (2)$$

$$Si\,(gas) \uparrow + SiC\,(solid) \Leftrightarrow Si_2C\,(gas) \uparrow \quad (3)$$

The silicon-carrying gas species play a role of a transport medium of carbon, silicon and silicon carbide. The gases diffuse in the porous sample under the gradients of the pressure and concentration. In the short-range distance, the pressure gradients (differential temperature) were produced by the decomposition and recrystallization of silicon carbide. In the long distance,

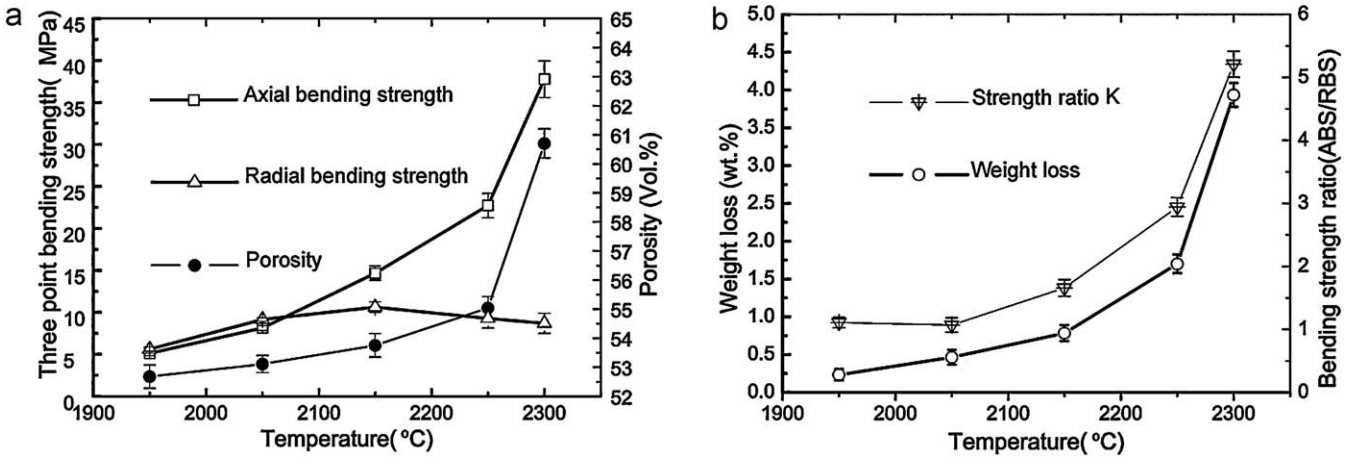

Fig. 6. The effect of the temperature variation on the anisotropic mechanical properties, porosities, and weight loss of samples: (a) the bending strength and porosities and (b) bending strength ratio *K* (ABS/RBS) and weight loss.

the differential pressures (concentration gradients) were mainly produced by the differential gas pressure between the inside and outside of the graphite sagger. The pressure and concentration gradients are two driving forces for the transport of mass (gases), and the direction of the gases flow depends on the pressure difference gradients. The maximum pressure difference was shown in the axial direction which drives the gases flow in the axial direction, and then moves upwards to the upper surface of the green body or migrate into the outside of the crucible through the gap among particles. When the pressure of gases is sufficient to overcome the diffusion resistance of gases, the anisotropic particles rearranged directionally in axial direction, and formed the aligned gas channels (pores) in the axial direction (Fig. 3).

The parts of gases leave the graphite sagger, which leads to the mass loss of samples. The degree of the mass loss (gases) reflects the changes of the amount of the directional mass transport along the axial direction. There is a positive relationship between the mass loss and the degree of directional pores (growth of SiC crystals) within a certain pressure and temperature ranges.

Based on the above analysis, the microstructure of porous silicon carbide strongly depends on the sintering temperature and the furnace pressure. In order to investigate the evolution of microstructure with temperature and pressure, we have investigated the microstructure and mechanical properties of samples sintered at the different temperatures and pressures.

3.3. The effect of temperature changes

Figs. 3 and 5 show the evolution of the microstructure with temperature. The samples were sintered under the furnace pressure of 0.5×10^5 Pa in argon atmosphere from 1950 °C to 2300 °C for 2 h. The temperature cannot exceed 2400 °C because it would lead to the severe decomposition of silicon carbide and the recrystallization becomes difficult to be controlled. When the sintering temperature is between 1950 °C and 2050 °C, silicon carbide grains were distributed disorderly and isolated. Fig. 5a and b shows that most of silicon carbide grains remain their anisotropy and irregular flake shape, but the surface ablation[34] and rearrangement[35] of silicon carbide grain occur in Fig. 5b. When the temperature reached up to 2150 °C, the silicon carbide grains began to interconnect each other and formed the disordered chains and directional pores in the samples. When the sintering temperature is above 2150 °C (Figs. 5d and 3), the aligned columnar silicon carbide crystals and tubular pores were observed in the axial section surface.

According to the literature,[36] the pressure and chemical species of gases were determined by the sintering temperature. When the temperature is between 1800 °C and 2150 °C, the pressure and concentration gradients of gases are very small and the recrystallization of silicon carbide can only occur on the particle surface in short distance, which only lead to the interconnection of silicon particles and cannot obtain the aligned pores. In the range of temperature from 2200 to 2300 °C, it intensifies the decomposition and recrystallization of silicon carbide. When the gases pressure difference between the inside and outside of the graphite sagger increases and overcomes the gases diffusion resistance, the anisotropic particles are directionally rearranged which leads to the mass directional transport of species (the Si, SiC and C) in the axial direction. The surface of silicon carbide grains was directionally eroded by the gas mixture, which formed the aligned pores and SiC crystals in the axial direction, and showed in Figs. 5d and 3.

Fig. 6 shows the effect of sintering temperature on the porosity, anisotropic mechanical properties and weight loss of samples. The porosity of samples increases with increasing the sintering temperature due to the loss of SiC particles that were decomposed into gases. Below 2150 °C, the axial bending strength is approximately equal to the radial bending strength because there are no directional pores and silicon carbide crystals in the sample in Fig. 5a and b. With increasing the sintering temperature, the axial bending strength is higher than the radial bending strength due to the formation of the aligned pores and crystals in the axial direction (see Figs. 5d and 3). *K* is the ratio of the axial bending strength (ABS) to the radial bending strength (RBS), which reflects the anisotropic mechanical properties of the porous silicon carbide ceramics. The porosity, weight loss and strength anisotropy of ceramics increased with increasing the sintering temperature from 1950 °C to 2300 °C, while the

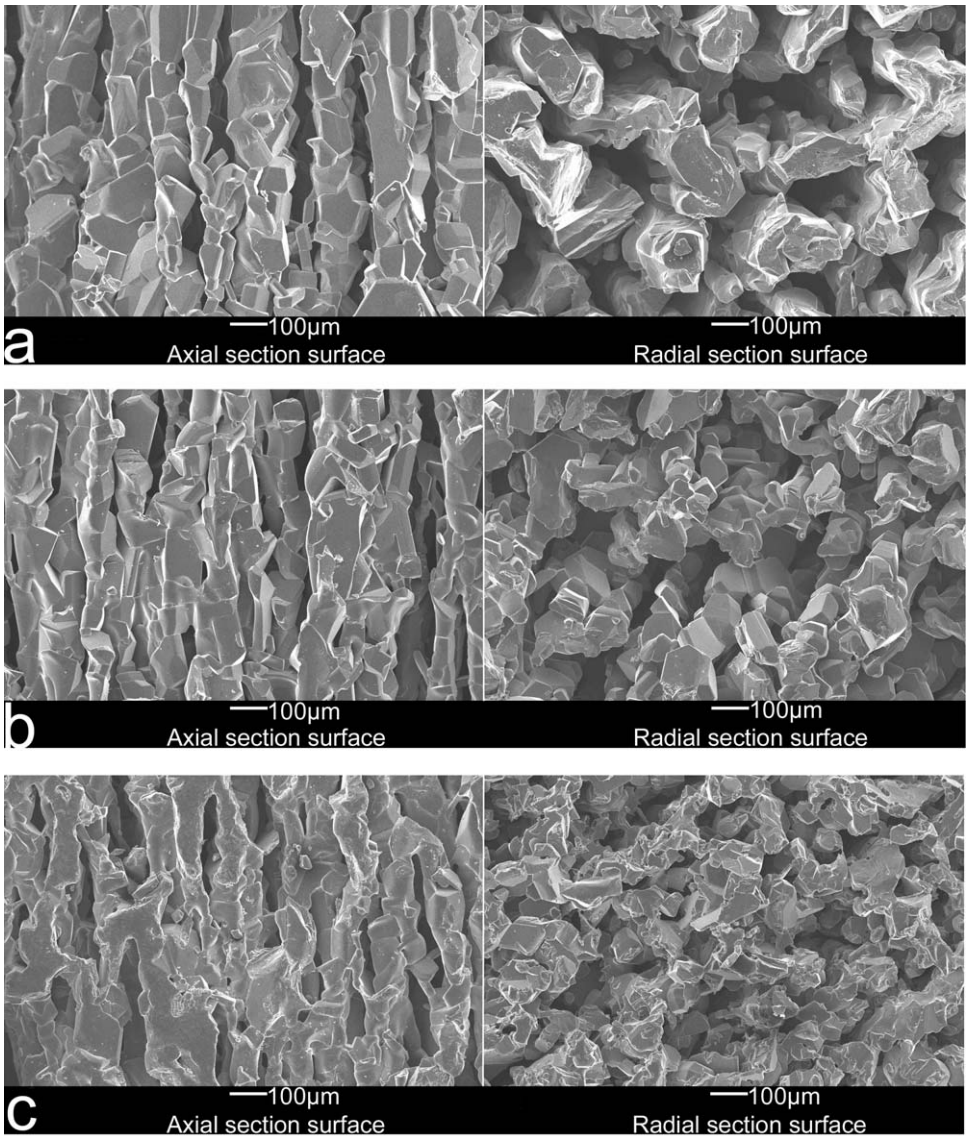

Fig. 7. The effect of the furnace pressure on the microstructure of samples (2250 °C, 2 h): (a) 0.3×10^5 Pa, (b) 0.4×10^5 Pa, and (c) 0.6×10^5 Pa.

mechanical properties of samples show the different change in the axial and radial directions.

3.4. The effect of furnace pressure changes

Fig. 7 shows the evolution of the microstructure of samples with the furnace pressure. The samples were sintered at 2250 °C for 2 h under the furnace pressure from 0.3×10^5 to 0.6×10^5 Pa in Ar atmosphere. As can be seen, the arrangement of silicon carbide crystals and pores strongly depend on the furnace pressure. When the furnace pressure is 0.3×10^5 Pa, the microstructures of samples display the highest orientation of silicon carbide crystals and pores in the axial direction (Fig. 7a). However, with increasing the furnace pressure, the degree of alignment decreases, such as the arrangement of silicon carbide crystals and pores become messy in the axial direction, and it also shows the low porosity and higher density under the furnace pressure of 0.6×10^5 Pa (Fig. 7c).

According to the decomposition reactions of SiC in Section 3.2 and the literature,[32,36–39] the furnace pressure influences the rates of the decomposition and recrystallization of silicon carbide. As the furnace pressure increases, the crystal nucleation will be enhanced and hence increase the recrystallization rate of silicon carbide crystals. Consequently, the pressure/concentration gradient decreased between the inside and outside of the graphite sagger, and leading to the decreases of the mass transport rate and the distance of mass transport. When the pressure of gases at the powder surface is greater than the equilibrium pressure of decomposed SiC gases, the SiC granule will stop decomposing, and the mass transport and SiC crystals growth will be interrupted. Thus, the porosity and strength anisotropy of ceramics decreased with increasing furnace pressure from 0.3×10^5 to 0.6×10^5 Pa at 2250 °C.

Fig. 8 shows the effect of the furnace pressure on the anisotropic mechanical properties, porosities and weight loss of samples. The porosities, weight loss and bending strength ratio K

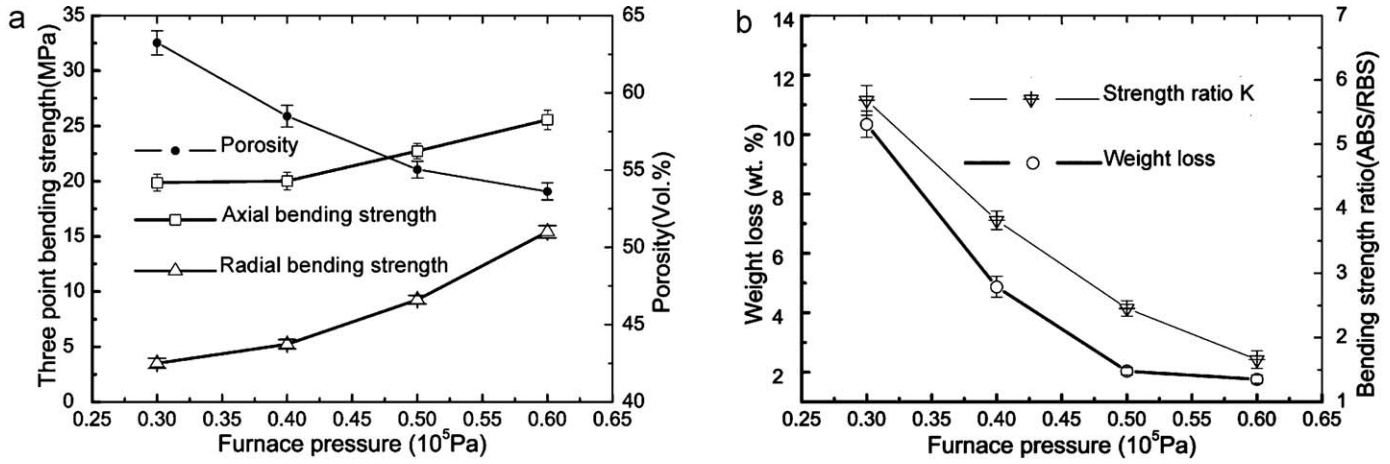

Fig. 8. The effect of the pressure on the anisotropic mechanical properties, porosities and weight loss of samples (2250 °C, 2 h): (a) the bending strength and porosities and (b) bending strength ratio *K* (ABS/RBS) and weight loss.

decrease with increasing the furnace pressure, while the bending strength increase. The anisotropy degree of ceramics decreases with increasing the furnace pressure, which result from the lowly aligned silicon carbide crystal in the axial direction and was confirmed by Figs. 7 and 5d.

4. Conclusions

The porous wood-like pure silicon carbide ceramics with the highly aligned silicon carbide crystals and high porosity were obtained when the samples were sintered at 2300 °C for 2 h under the furnace pressure of 0.5×10^5 Pa or at 2250 °C for 2 h under the furnace pressure of 0.3×10^5 Pa in argon atmosphere. The microstructures and properties of porous silicon carbide strongly depend on the sintering temperature and furnace pressure. Silicon carbide decomposes to produce the gas mixture at high temperature. The directional flow of mixture gases along the axial direction induces the surface ablation and rearrangement of silicon carbide grains, which leads to the formation of the directional columnar silicon carbide crystals and tubular pores in the axial direction of samples within a certain pressure and temperature range.

References

1. Vogta UF, Györfy L, Herzoga A, Graule T, Plesch G. Macroporous silicon carbide foams for porous burner applications and catalyst supports. *J Phys Chem Solids* 2007;**68**:1234–8.
2. Withers CJ, West AA, Twigg AN, Courtney RS, Seville JPK, Clift R. Improvements in the performance of ceramic media for filtration of hot gases. *Filtr Sep* 1990;**27**:32–4.
3. Lee JS, Lee SH, Choi SC. Improvement of porous silicon carbide filters by growth of silicon carbide nanowires using a modified carbothermal reduction process. *J Alloys Compd* 2009;**467**:543–9.
4. Zhu SM, Ding SQ, Xi HA, Wang RD. Low-temperature fabrication of porous SiC ceramics by preceramic polymer reaction bonding. *Mater Lett* 2005;**59**:595–7.
5. Liu SF, Zeng YP, Jiang Dl. Fabrication and characterization of cordierite-bonded porous SiC ceramics. *Ceram Int* 2009;**35**:597–602.
6. Gain AK, Han JK, Jang HD, Lee BT. Fabrication of continuously porous SiC–Si_3N_4 composite using SiC powder by extrusion process. *J Eur Ceram Soc* 2006;**26**:2467–73.
7. Maitya A, Kalitab D, Kayala TK, Goswamib T, Chakrabartia Q, Maitia HS, et al. Synthesis of SiC ceramics from processed cellulosic bio-precursor. *Ceram Int* 2010;**36**:323–31.
8. Pancholia V, Mallickb D, AppaRaoc Ch, Samajdara P, Chakrabartib OP, Maitib HS, et al. Microstructural characterization using orientation imaging microscopy of cellular Si/SiC ceramics synthesized by replication of Indian dicotyledonous plants. *J Eur Ceram Soc* 2007;**27**:367–76.
9. Sieber H, Hoffmann C, Kaindl A, Greil P. Biomorphic cellular ceramics. *Adv Eng Mater* 2000;**2**:105–9.
10. Harris AT, Maddocks AR. Synthesis of porous silicon carbide from cellulose fibre templates infiltrated with polycarbosilane. *J Mater Sci Technol* 2010;**26**:375–8.
11. Ghanem H, Gerhard H, Popovska N. Paper derived SiC–Si_3N_4 ceramics for high temperature applications. *Ceram Int* 2009;**35**:1021–6.
12. Luo M, Gao JQ, Qao GJ. Synthesis of wood-derived ceramics from biological templates. *Prog Chem* 2008;**20**:989–1000.
13. Zhu JT, Kwong FL, Ng DHL. Synthesis of biomorphic SiC ceramic from bamboo charcoal. *J Nanosci Nanotechnol* 2009;**02**:1564–7.
14. Kiselov VS, Kalabukhova EN, Sitnikov AA, Lytvyn PM, Poludin VI, Yukhymchuk VO, et al. Effect of Si infiltration method on the properties of biomorphous SiC. *Semicond Phys Quant Electron Optoelectron* 2009;**12**:68–71.
15. Greil P, Lifka T, Kaindl A. Biomorphic cellular silicon carbide ceramics from wood: I. Processing and microstructure. *J Eur Ceram Soc* 1998;**18**:1961–73.
16. Greil P, Lifka T, Kaindl A. Biomorphic cellular silicon carbide ceramics from wood: II. Mechanical properties. *J Eur Ceram Soc* 1998;**18**:1975–83.
17. Singh M, Salem JA. Mechanical properties and microstructure of biomorphic silicon carbide ceramics fabricated from wood precursors. *J Eur Ceram Soc* 2002;**22**:2709–17.
18. Vogli E, Sieber H, Greil P. Biomorphic SiC–ceramic prepared by Si-vapor phase infiltration of wood. *J Eur Ceram Soc* 2002;**22**:2663–8.
19. Fernández JM, Munoz A, Lopez ARDA, Feria FMV, Dominguez-Rodriguez A, Singh M. Microstructure–mechanical properties correlation in siliconized silicon carbide ceramics. *Acta Mater* 2003;**51**:3259–75.
20. Zink-Sharp A. *Wood formation and properties, Formation and structure of wood. Encyclopedia of forest sciences*. Kensington, England: Elsevier Academic; 2004. p. 1806–15.
21. Plomion C, Leprovost G, Stokes A. Wood formation in trees. *Plant Physiol* 2001;**127**:1513–23.
22. Boura A, Franceschi DD. Is porous wood structure exclusive of deciduous trees? *CR Palevol* 2007;**6**:385–91.

23. Meinzer FC, Clearwater MJ, Goldstein G. Water transport in trees: current perspectives, new insights and some controversies. *Environ Exp Bot* 2001;**45**:239–62.
24. Pedersona N, Cookb ER, Jacobyb GC, Peteetc DM, Griffin KL. The influence of winter temperatures on the annual radial growth of six northern range margin tree species. *Dendrochronologia* 2004;**22**:7–29.
25. Mandal PK, Majumdar R, Mukherjee KK, Chakrabarti O, Maiti HS. Active cellular preform derived from stems of jute and sticks of cane and their suitability for bulk porous Si/SiC ceramics. *J Porous Mater* 2009;**16**:157–63.
26. Shpeizman VV, Peschanskaya NN, Orlova TS, Smirnov BI. Microplasticity of biomorphic SiC/Al composite under uniaxial compression. *Phys Solid State* 2009;**51**:2458–62.
27. Willa J, Hoppea A, Müllerb FA, Rayac CT, Fernándezc JM, Greila P. Bioactivation of biomorphous silicon carbide bone implants. *Acta Biomater* 2010:036, doi:10.1016/j.actbio.2010.06.
28. Hofenauer A, Treusch O, Tröger F, Wegener G, Fromm J, Gahr M, et al. Dense reaction infiltrated silicon/silicon carbide ceramics derived from wood based composites. *Adv Eng Mater* 2003;**5**:794–9.
29. Mallick D, Chakrabarti OP, Maiti HS, Majumdar R. Si/SiC ceramics from wood of Indian dicotyledonous mango tree. *Ceram Int* 2007;**33**:1217–22.
30. Sudarshan TS, Maximenko SI. Bulk growth of single crystal silicon carbide. *Microelectron Eng* 2006;**83**:155–9.
31. Duquenne P, Deltour A, Lacoste G. Application of inductive heating to granular media: modelling of electrical phenomena. *Can J Chem Eng* 1994;**72**:975–81.
32. Lilov SK. Study of the equilibrium processes in the gas phase during silicon carbide sublimation. *Sci Eng B* 1993;**21**:65–9.
33. Li H, Chen XL, Ni DQ, Wu X. Factors affecting the graphitization behavior of the powder source during seeded sublimation growth of SiC bulk crystal. *J Cryst Growth* 2003;**258**:100–5.
34. Kulik AV, Bogdanov MV, Karpov SY, Ramm MS, Makarov YN. Theoretical analysis of the mass transport in the powder charge in long-term bulk SiC growth. *Mater Sci Forum* 2004;**457–460**:67–70.
35. Exnerw HE, Müller C. Particle rearrangement and pore space coarsening during solid-state sintering. *J Am Ceram Soc* 2009;**92**:1384–90.
36. Hofmanna D, Ecksteina R, Kölbla M, Makarovb Y, Müllera SG, Schmitta E, et al. SiC-bulk growth by physical-vapor transport and its global modelling. *J Cryst Growth* 1997;**174**(1–4):669–74.
37. Lilov SK. Peculiarities of silicon carbide crystal growth in quasi closed volume. *Cryst Res Technol* 1993;**28**:299–303.
38. Tairov YM. Growth of bulk SiC. *Mater Sci Eng B* 1995;**29**:83–9.
39. Liu X, Chen BY, Song LX, Shi EX, Chen ZZ. The behavior of powder sublimation in the long-term PVT growth of SiC crystals. *J Cryst Growth* 2010;**312**:1486–90.